Geomorphology 360 (2020) 107164

Contents lists available at ScienceDirect

Geomorphology

journal homepage: www.elsevier.com/locate/geomorph

Controls on jökulhlaup-transported buried ice melt-out at Skeiðarársandur, Iceland: Implications for the evolution of ice-marginal environments

David J. Blauvelt [a], Andrew J. Russell [a,*], Andrew R.G. Large [b], Fiona S. Tweed [c], John F. Hiemstra [d], Bernd Kulessa [d,e], David J.A. Evans [f], Richard I. Waller [g]

[a] 116 East Glebe Rd, Alexandria, VA 22305, USA
[b] Newcastle University, School of Geography Politics and Sociology, NE1 7RU, UK
[c] Geography, Staffordshire University, College Road, Stoke-on-Trent, ST4 2DE, UK
[d] College of Science, Swansea University, Singleton Park, SA2 8PP, Wales, UK
[e] School of Technology, Environments and Design, University of Tasmania, Hobart, Tasmania 7001, Australia
[f] Department of Geography, Durham University, Lower Mountjoy, South Road, Durham DH1 3LE, UK
[g] School of Geography, Geology and the Environment, Keele University, Staffordshire ST5 5BG, UK

ARTICLE INFO

Article history:
Received 29 November 2019
Received in revised form 10 March 2020
Accepted 10 March 2020
Available online xxxx

Keywords:
Jökulhlaup
Buried ice melt-out
Skeiðarársandur Iceland
Icemarginal environments

ABSTRACT

High-magnitude jökulhlaups, glacier margin position and ice-thickness have been identified as key controls on sandur evolution. Existing models however have focused primarily on observations made during short windows of time and often do not account for the subsequent modification of proglacial landsystems by repeated jökulhlaups or post-depositional modification due to melt out over decadal time-scales. Digital Elevation Models (DEMs) were used to reconstruct the development of large depressions on Skeiðarársandur, an outwash plain in southeast Iceland. These depressions measure up to 1 km in width and up to 13 m in depth and are associated with ice bodies up to 1 km in length and up to 150 m in height emplaced during a high-magnitude jökulhlaup in 1903 and subsequently buried by jökulhlaups in 1913 and 1922. The continued melting of the Harðaskriða ice bodies over a century following their emplacement, together with subsequent repeated burial, by high-magnitude jökulhlaups demonstrates that jökulhlaups may continue to serve as important controls on sandur evolution on a decadal to centennial timescale (10^1–10^2 years). The Harðaskriða depressions developed only following the retreat of the glacier margin after 1945, which highlights the controls of margin position on the evolution of the sandur. Margin position and thickness of the glacier profile was seen to affect not only the distribution and thickness of sediment emplaced during jökulhaups but also the rate and pattern of melt in the decades following the decoupling of the margin from the sandur. The jökulhlaup landsystem model signatures identified at this site may provide a useful analogue for interpreting landforms and strata emplaced by glacier margin fluctuations, jökulhlaups and melt out generated by retreating continental Pleistocene ice sheets.

1. Introduction

Glaciers are frequently used as indicators of climate change as they respond dynamically to changes in the climate driven components of their mass balance. Knowledge of the former extent of glaciers can be used to reconstruct palaeo-climate and to define the former position of contemporary glaciers. Distinctive assemblages of landforms and deposits at modern glacier-margins have stimulated the development of models which can be used to reconstruct ice-marginal processes. Models such as the ice-marginal landsystem (e.g. Krüger, 1994; Evans and Twigg, 2002; Evans et al., 2019) were developed from the detailed investigation of contemporary glacier margins and have been used to reconstruct palaeo-glacier margins in the Quaternary record (e.g. Evans et al., 1999). By definition, many studies of contemporary ice-marginal processes provide only a snapshot of the geomorphological and sedimentological evolution of an ice-marginal zone, as they do not take account of post-depositional landscape modification processes and are not always able to constrain the influences of previous landsystems on landscape evolution. Palimpsest landscapes comprising a number of superimposed landsystems allow landform overprinting and the potential for landsystem legacy to persist for periods of 10^1–

* Corresponding author.
E-mail address: andy.russell@ncl.ac.uk (A.J. Russell).

https://doi.org/10.1016/j.geomorph.2020.107164
0169-555X/

10^2 yr^{-1} modifying subsequent landsystems (Kleman, 1992; Kleman and Stroeven, 1997; Schomacker and Kjær, 2007; Korsgaard et al., 2015).

Ice-marginal and proglacial geomorphology can be modified by a number of post-depositional processes such as aeolian deflation and deposition, fluvial erosion and deposition, periglacial and paraglacial slope processes (e.g. Ballantyne, 2002; Mountney and Russell, 2006, 2009). Melt-out of buried glacier ice has been well-documented from modern ice-margins (Price, 1969; Schomacker and Kjær, 2007; Tonkin et al., 2016) as well as being interpreted from the Quaternary record (Eyles et al., 1999; Fard, 2003). Buried ice melt-out has been invoked to account for a number of distinctive landforms such as 'kame and kettle' topography and 'hummocky moraine', both of which result from topographic inversion as buried ice melts, causing slow collapse of overlying sediment (e.g. Everest and Bradwell, 2003; Lukas et al., 2005; Bennett and Glasser, 2009).

Despite widespread acknowledgement of the importance of buried ice within former glacier margins, relatively little attention has been paid to the process of ice emplacement and how this may determine buried ice distribution and melt-out styles. Studies of buried ice melt out also tend to have focused on the immediate ice proximal areas of proglacial outwash plains. Similarly, there are scant data on the rates of ice melting beneath thick debris mantles; exceptions include McKenzie (1969) and Schomacker (2008). Buried ice is known to have survived for decades to centuries (e.g. French and Harry, 1990; Evans and England, 1992; Everest and Bradwell, 2003; Schomacker, 2008) however there have been few detailed studies of melt-out rates over these timescales.

Processes occurring in the ice-marginal zones of glaciers and ice sheets are complex. Subaerial processes re-work glacially-deposited debris and the melt-out of buried ice leads to collapse structures and topographic inversion (Price, 1969; Bennett and Glasser, 2009). Even a thin (>0.01 m) layer of debris covering glacier ice can provide sufficient insulation to retard ablation (e.g. Lister, 1953; Østrem, 1959; Nakawo and Young, 1981, 1982; Nicholson and Benn, 2006) and ablation can be very slow under thick debris mantles. Very slow melt rates can therefore permit the survival of buried glacier ice for long periods of time. The sustained collapse of overlying sediment due to buried ice melt-out is a significant post-depositional modification process in deglaciated landscapes with ice-cored topography (Ballantyne, 2002). The correlation between climatic parameters and melt rates of buried ice bodies is weak however, suggesting that both burial processes and topography play a key role in the rates of ice melting (Nicholson and Benn, 2006; Schomacker, 2008).

Glacier ice can also be buried 'in situ' by supraglacial sediment deposition on top of an active or stagnant glacier margin (e.g. Russell and Knudsen, 2002; Schomacker and Kjær, 2007; Schomacker et al., 2006). During jökulhlaups, ice blocks become detached by englacial hydrofracturing, meltwater conduit collapse and ice cliff collapse (Roberts et al., 2000; Roberts, 2005). Ice-blocks up to 10^2 m in diameter are known to have been washed from glacier margins by jökulhlaups on to outwash plains (sandar) and subsequently either partially or completely buried by sandur aggradation (Tómasson, 1996; Russell and Knudsen, 1999; Roberts et al., 2000; Fay, 2001, 2002a, 2002b; Roberts, 2005; Russell et al., 2006). Melt out of ice blocks transported by the 2010 Eyjafjallajökull eruption generated jökulhlaups is thought

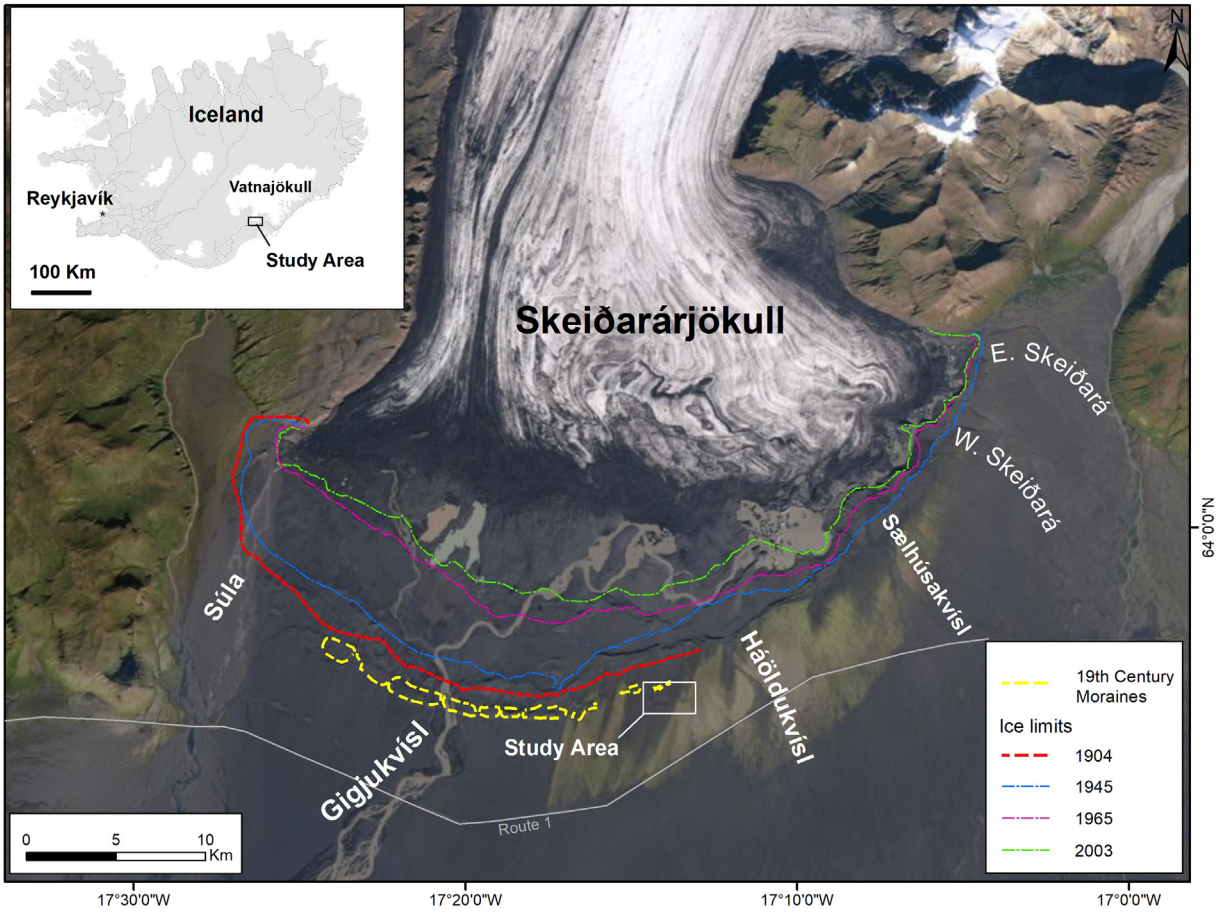

Fig. 1. Skeiðarárjökull in Iceland (top inset) and its margin showing , the retreat of the margin since 1945, the location of the 19th century moraines and the major proglacial river channels (Imagery: 2010 Google Earth; Iceland inset - Justus Lyons).

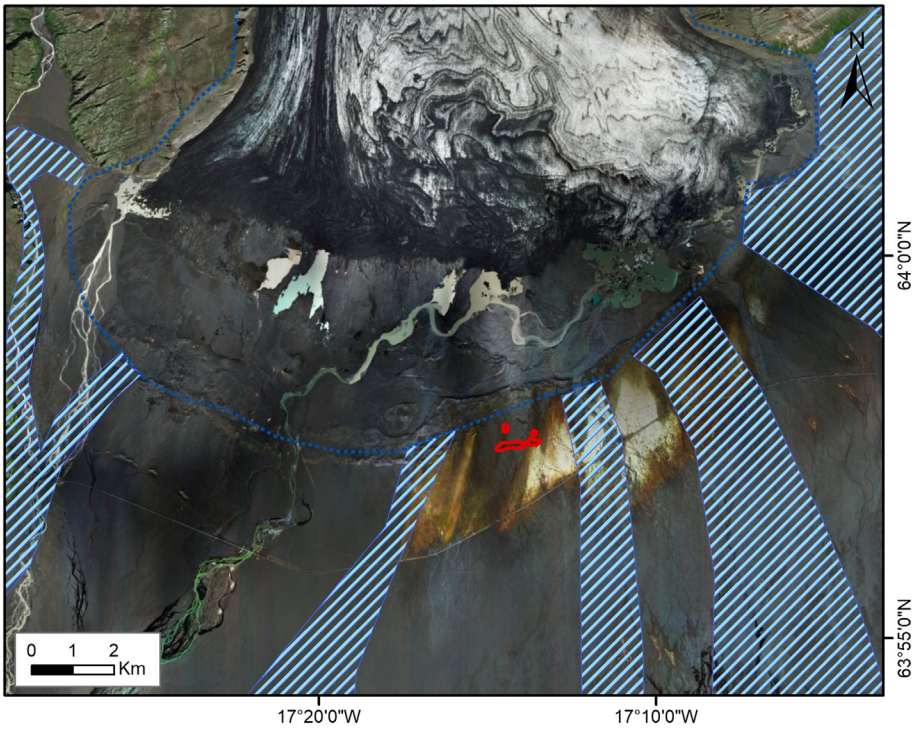

Fig. 2. Approximate extent of 1934 ice margin (dashed blue line) and location of jökulhlaup routing (blue hashed polygons) on top of 2016 Digital Globe photomosaic. Red polygons delineate location of depressions (Thórarinsson, 1974). (For interpretation of the references to colour in this figure legend, the reader is referred to the web version of this article.)

to have played a major role in post depositional landscape evolution (Harrison et al., 2019).

During the November 1996 jökulhlaup, ~8.3 × 10^6 m^3 of ice was removed from Skeiðarárjökull (Fay, 2002a, 2002b; Russell et al., 2001a, 2005). Sections of the snout of Skeiðarárjökull were fractured in situ into blocks up to 200 m × 400 m in size (Roberts et al., 2000). Ice blocks as large as 45 m in diameter were transported from the glacier margin (Fay, 2002a, 2002b; Russell et al., 2005). Some of these ice blocks were deposited as a linear jökulhlaup flow-parallel cluster, resulting in a single coalesced kettle hole approximately 130 m wide and 40 m long (Fay, 2002a; Russell and Knudsen, 1999, 2002). The largest accumulation of ice blocks was over 1 km in length with a width of up to 300 m (Fay, 2002a; Russell and Knudsen, 2002). Ice blocks transported and buried by such single high-magnitude jökulhlaups are known to persist for 10^1–10^2 yr^{-1} (e.g. Fay, 2002a, 2002b; Everest and Bradwell, 2003; Russell et al., 2005).

The aims of this paper are to: (1) determine the origin of a series of actively developing depressions within the proglacial area of

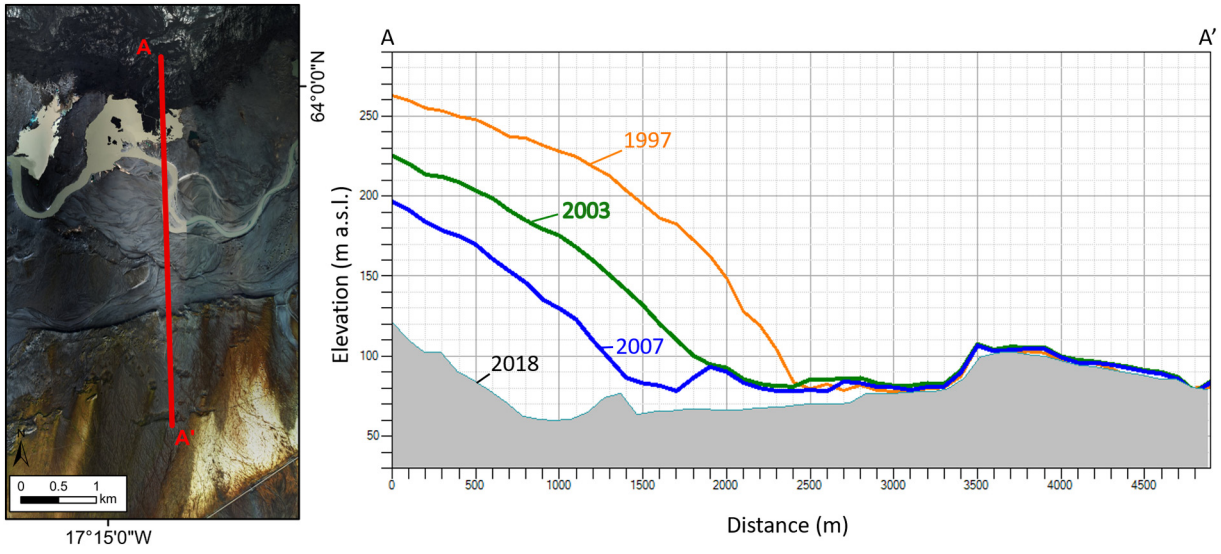

Fig. 3. Proximal to distal profiles of the glacier and the sandur, demonstrating the retreat of the margin and the base level lowering of drainage within the proglacial depression, and assumed lowering of groundwater table. The 1997, 2003, 2007 profiles are derived DEMs from imagery acquired by Landmælingar Íslands, Loftmyndir ehf. and NERC ARSF, respectively. The 2018 profile is derived from ArcticDEM.

Skeiðarársandur, southeast Iceland; (2) evaluate the mode and significance of buried ice emplacement and subsequent melt for depression development; and (3) explain their significance for sandur evolution. To fulfil these aims we quantify the decadal evolution of the depressions and characterise their sub-surface sedimentary architecture and relate to the wider record of jökulhlaups on Skeiðarársandur.

2. Study area

Harðaskriða is located 3.6 km from the current margin of Skeiðarárjökull within the central zone of Skeiðarársandur, a 1300 km^2 outwash plain fed by Skeiðarárjökull in southeast Iceland (Fig. 1). Skeiðarárjökull is a temperate, surge-type, outlet glacier of Vatnajökull ice cap with a 23 km wide piedmont snout (Björnsson, 1998). Skeiðarársandur has a strong maritime climate, where the maximum depth of winter freezing is only of the order of centimetres (Douglas and Harrison, 1996; Thórhallsdóttir, 1996) making the presence of permafrost impossible. Skeiðarárjökull and Skeiðarársandur have been subject to repeated high-magnitude jökulhlaups generated both by subglacial volcanic eruptions and the drainage of subglacial and ice-marginal lakes (Thórarinsson, 1974; Björnsson, 1992, 1997). The Harðaskriða area of Skeiðarársandur last experienced meltwater flow during the 1922 jökulhlaup, after which glacier margin recession created incised proglacial channels at the Háöldukvísl and Gígjukvísl; subsequently a proglacial trench developed, allowing all subsequent meltwater to be routed westward (Galon, 1973) (Figs. 2, 3 and 4; Table 1). The Harðaskriða area is now part of an elevated sandur surface which was unaffected by the large November 1996 jökulhlaup (Snorrason et al., 2002). The Harðaskriða area was however inundated by eleven large jökulhlaups between 1861 and 1938 when Skeiðarárjökull was at its Little Ice Age maximum extent (Thórarinsson, 1974; Björnsson, 1997; Glaciorisk, 2005) (Table 1). These high frequency high-magnitude jökulhlaups resulted in significant aggradation on the eastern and central proximal areas of Skeiðarársandur with accumulated elevations of up to ~125 m above sea level (a.s.l.) compared with elevations of below 90 m a.s.l. for equivalent-aged sandur surfaces to the west (Blauvelt, 2013). Historic accounts indicate a number of large jökulhlaups associated with glacier margin disruption and ice block release in the Harðaskriða area between 1861 and 1938 (Thórarinsson, 1974; Glaciorisk, 2005) (Fig. 2; Table 1). The 1897 and 1903 jökulhlaups can also be specifically linked to the Harðaskriða area (Thórarinsson, 1974). A 1 km long, 150 m high piece of the glacier margin was washed out on to the sandur during the 1903 jökulhlaup possibly associated with detachment along a large, ice flow transverse, hydrofracture generating a large 'embayment' (Roberts et al., 2000; Roberts, 2005).

The Harðaskriða comprises outwash surfaces characterised by a well-developed channel and bar pattern supporting numerous ice block obstacle marks up to 10 m in diameter (Fig. 4). These outwash surfaces are however disrupted by four large depressions the largest of which has maximum dimensions of 604 × 108 m and a depth of ~13 m (Figs. 5, 6 and 7). Although there are historic accounts of high magnitude jökulhlaup processes and immediate impacts at Harðaskriða there has been no detailed examination of the development of the resulting landforms and deposits.

3. Methods

3.1. Topographic survey and DEM generation

DEMs for 1968 and 2007 were produced using stereophotogrammetry on digital aerial imagery. Vertical aerial photographs collected for DEM creation were obtained from the National Land Survey of Iceland, Landmælingar Íslands. Images were scanned by Landmælingar Íslands with an Eversmart Jazz+ Scitex scanner, at a resolution of 2000 dpi and delivered as tagged image format (tif) files. Camera calibration documentation and flight lines drawn on 1:100,000 topographic maps were provided for all photographs taken after 1954. Photographs from 1945, taken by the U.S. Air Force, were purchased from Landmælingar Íslands, who provided known flight

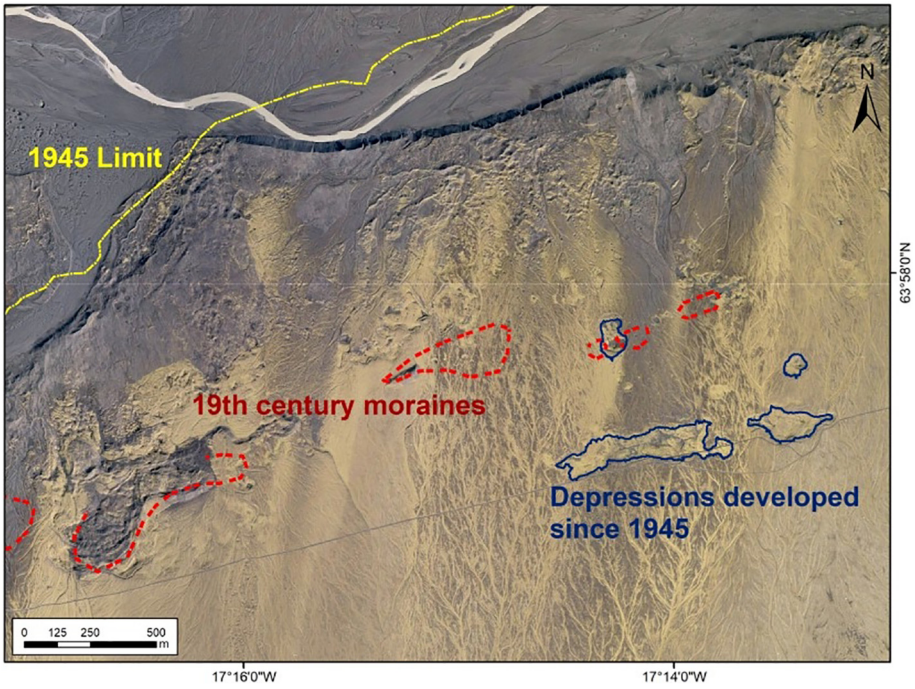

Fig. 4. Approximate locations of 19th century moraines estimated from georeferenced 1904 topographic map (red line) on 2003 imagery. Blue indicates depressions that have developed since 1945. (For interpretation of the references to colour in this figure legend, the reader is referred to the web version of this article.)

Table 1
Chronology of glacier margin fluctuations and jökulhlaups (1598–1954) from the drainage of Grímsvötn subglacial lake draining from Skeiðarárjökull. Information in this table is sourced from Thórarinsson (1974), Björnsson (1997), Glacier risks database (2005) and Ives (2007).

Year	Eruption	Glacier margin advance/recession	Jökulhlaup impacts *(Impacts on the Harðaskriða area)*
1598	Yes	Advance	No detailed information available.
1629	Yes	Advance	Huge jökulhlaup with at least five enormous flood paths across Skeiðarársandur. Fertile land flooded, one family died and at least one man isolated 5 days on a high hill in the flood area.
1816	?	Little Ice Age Maximum	No detailed information available.
1838	?	Little Ice Age Maximum	No detailed information available.
1851	Yes	Little Ice Age Maximum	No detailed information available.
1861	Yes?	Little Ice Age Maximum	Large jökulhlaup (Stórahlaup) which destroyed much land close to the farms Svínafell, Hof and Hofsnes. Icebergs and large quicksand areas (kettle holes) formed in the flood path.
1867	Yes	Little Ice Age Maximum	Large jökulhlaup, 13 days duration, waning on the 4th day. Icebergs washed out onto Skeiðarársandur, which was completely covered by water.
1873	Yes	Little Ice Age Maximum	Fairly small jökulhlaup. The discharge in the river Súla increased right after the beginning of the jökulhlaup in river Skeiðará.
1883	yes	Little Ice Age Maximum	No detailed information available.
1892	Yes?	Little Ice Age Maximum	One of the largest jökulhlaups in river Skeiðará with a duration of four days. Peak discharge reached after two days accompanied by tremendous noise. The next day ice blocks were covering the sandur all the way to the ocean. Ice blocks were up to 20 m in diameter and very tightly packed. South of the main flood outlet, icebergs, up to 20 m high, covered a 7 km wide region. Mud was spread over the flooded area and was unusually thick. Melting icebergs and quicksand made it difficult to cross the Skeiðarársandur for several months after the flood.
1897	Yes	Little Ice Age Maximum	This jökulhlaup was smaller than the one in 1892 and had a duration of 10 days with a 6 day rising stage. It burst from Skeiðarárjökull near Harðaskriða, a steep moraine south of central Skeiðarárjökull. Ice blocks up to 20 m in diameter were spread over a 6 km wide area between Harðaskriða and the Skeiðará. ***(Potential source of jökulhlaup transported ice blocks to the Harðaskriða area).***
1903	Yes		Large jökulhlaup with a duration of 4 days reaching discharge peak very quickly and covering more of the western outwash plain than usual. Ice blocks were carried all the way to the ocean. A large piece of the glacier margin detached during the 1903 jökulhlaup approximately 1 km in length and up to 150 m in height; it was also documented that a fracture of similar size and length developed up glacier located where the floodwaters burst from the glacier margin. ***(Potential source of jökulhlaup transported ice blocks to the Harðaskriða area).***
1913	No	Recession	Large jökulhlaup of 12 days duration. The flood was focussed on the eastern part of Skeiðarársandur. Large amounts of ice detached from snout of Skeiðarárjökull with ice blocks described as being the size of houses.
1922	Yes	Recession	This large jökulhlaup had a duration of 14 days and had its main outlet on the eastern side of Skeiðarársandur. Rising stage discharge increased slowly for 6 days before any ice blocks were observed being transported downstream. Followed by 8 days of recession. The jökulhlaup waned within one day. ***(Potential for aggradation in the Harðaskriða area).***
1934	Yes	Recession	A large jökulhlaup with a volume of 4.5 km^3 with a 16 day duration and a peak discharge of 25,000 to 30,000 m^3s^{-1}. The eastern most outlet was 2.5 km wide and ice blocks carried to ocean. ***(Potential for aggradation in the Harðaskriða area).***
1938	Yes	Recession	A large jökulhlaup with a volume of 4.7 km^3, a peak discharge of 25,000 to 30,000 m^3s^{-1} and a 16 day duration. Almost all Skeiðarársandur was flooded with ice blocks covering the sandur, although they were smaller than those generated by the 1934 jökulhlaup. ***(Potential for aggradation in the Harðaskriða area).***
1941	No	Recession	A small jökulhlaup with a duration of 17 days and a volume of 1.4 km^3. Relatively small ice blocks released from the glacier snout. ***(No impact on the Harðaskriða area due to the formation of a proglacial trench diverting flow in a westward direction).***
1945	No	Recession	A jökulhlaup with a duration of 12 days, a volume of 2.6 km^3 and a peak discharge of 10,000 m^3s^{-1}. Jökulhlaup flowed in the Skeiðará, Sandgígjukvísl and Núpsá river and produced relatively small ice blocks. ***(No impact on the Harðaskriða area due to the formation of a proglacial trench diverting flow in a westward direction).***
1948	No	Recession	A jökulhlaup with a duration of 17 days, a volume of 2.2 km^3 and a peak discharge of 5000 m^3s^{-1}. ***(No impact on the Harðaskriða area due to the formation of a proglacial trench diverting flow in a westward direction).***
1954	No	Recession	A jökulhlaup with a duration of 14 days, a volume of 3.2 km^3 and a peak discharge of 10,000 m^3s^{-1}. Jökulhlaup flowed in the Skeiðará and Sandgígjukvísl with peak discharges of 6000 m^3s^{-1} 4000 m^3s^{-1} respectively. ***(No impact on the Harðaskriða area due to the formation of a proglacial trench diverting flow in a westward direction).***

elevations and camera focal lengths. Colour digital images acquired in 2007 by NERC ARSF (IPY07/13) were also used in this study. Digital elevation models (20 m resolution) and photo mosaics were purchased from Loftmyndir HF for 1997 and 2003 datasets.

A differential GPS (dGPS) survey was conducted in 2007 between the glacier margin and Iceland's ring road (Fig. 1). Transects of four of the Harðaskriða depressions were surveyed (Fig. 7). Additionally, large-scale, persistent features across Skeiðarársandur including kettle holes, boulders and ridges that were visible on all historical aerial photographs were utilised for ground control points (GCPs). Survey points were collected using a Thales ProMark III unit, corrected to Icelandic Roads Authority survey sites.

BAE's *SocetSet* 5.5 (*Ngate*) software was used to generate the DEMs. Triangulation (interior and exterior orientation) was accomplished for all photosets. Once an internal coordinate system was established within the photographs, the control points measured in the field could be used to relate the image to the ground (absolute orientation). The ISN93 coordinates of the GCPs were used to identify points on the images. Once the x, y and z values of GCPs were identified on both (or more) images, SocetSet then performed point measurement automatically, using digital image matching (Baily et al., 2003).

Systematic errors and random errors were evaluated by comparing apparent elevation differences between the DEMs and ground control points measured with the dGPS. The location of the check points and ground control points are summarised in Table 2. Systematic errors are given as root-mean-square error (RMS) measures and the 95th percentile limit is given for random errors a technique commonly used in DEM quality analysis (Schiefer and Gilbert, 2007). All units are in metres above sea level (m a.s.l.). Following manual clean up ('post pushing') of the study area, all check points fell under 1 m. Due to the comparatively small scale and dynamic terrain of the study area, no additional registration was applied.

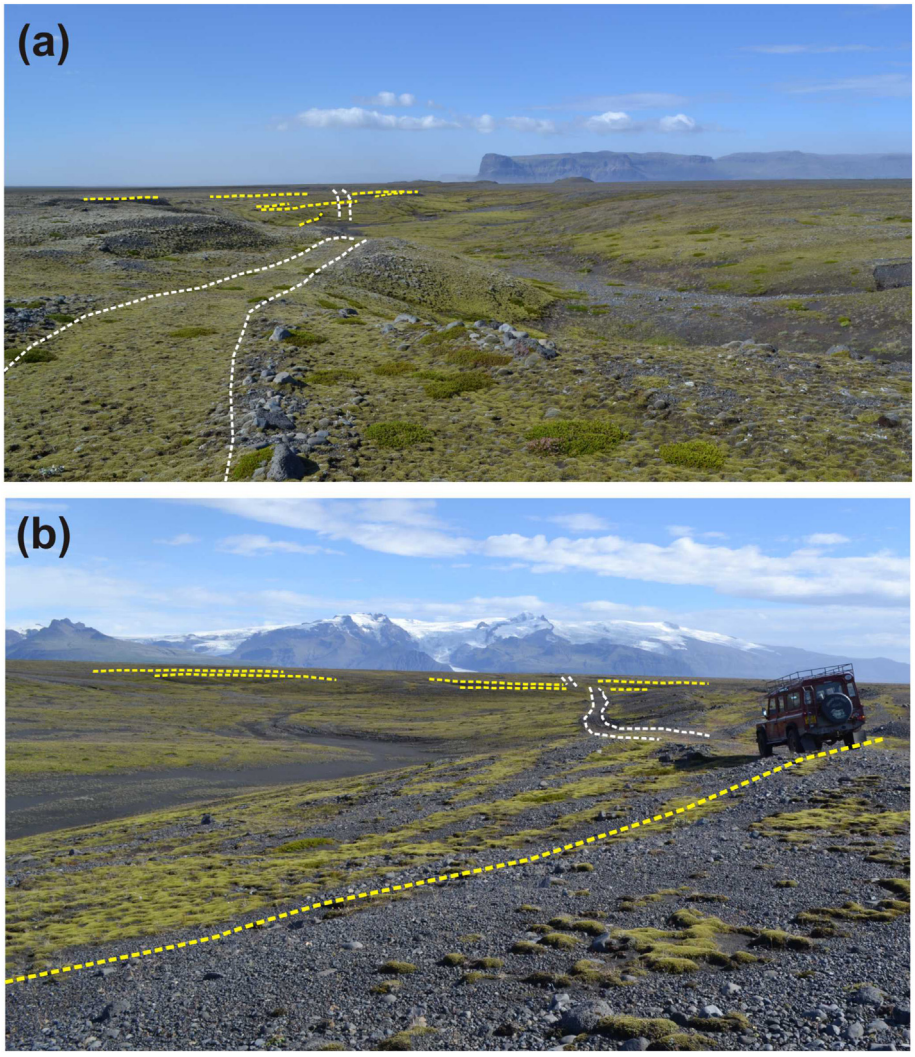

Fig. 5. (a) Top. A view towards the west of depression 4 (for location see Figs. 2 & 4). The upper surfaces of well-defined normally faulted blocks are indicated by the yellow dashed lines. The path of the old gravel road is indicated by the white dashed lines indicating substantial deformation and subsidence. (b) View towards the east of depression 4 showing concentric rings associated with individual fault blocks indicated by yellow lines. The path of the old gravel road is indicated by the white dashed lines indicating substantial deformation and subsidence. (For interpretation of the references to colour in this figure legend, the reader is referred to the web version of this article.)

Elevation differences were used to provide an approximate estimate of the volumetric loss for four of the major Harðaskriða depressions (Fig. 8) and the elevation loss of the adjoining glacier (Fig. 3). Whilst the poor quality of the 1945 images precluded the production of a 1945 DEM surface to quantify subsidence over the last sixty-two years, an attempt was made to provide as close an approximation as possible. Comparing surfaces constructed from two subsequent time periods (before and after) is often utilised as a cost-effective method to quickly quantify large-scale volumetric changes due to melt out, subsidence, flooding, human interference or other causes (Schiefer and Gilbert, 2007). By removing elevation points that lay within the depressions on the 2007 imagery and generating a triangular irregular network, or TIN, across the missing data points, a 1945 DEM surface could be simulated.

Although the 2018 ArcticDEM was used to provide a general comparison of glacier recession and proglacial fluvial system incision (Porter and 28 others, 2018) (Fig. 3), offsets between the 2018 ArcticDEM and photogrammetrically-derived DEMs, as well as the difficulty in removing bias in this type of terrain, precluded its use for quantification of rates of lowering of the Harðaskriða depressions.

3.2. Ground Penetrating Radar survey

Ground-Penetrating Radar (GPR) profiles were collected from depression 4 (Figs. 5 and 6) using the MALÅ ProEx system with a 13 m long (distance Tx – Rx = 6 m), low-frequency (30 MHz) Rough Terrain Antenna (RTA). GPR-lines (all corrected for topography), both outside and across the depression, were collected in 2013 (i.e. 6 years after the GPS surveys). The objectives were to gain insight in the subsurface sediment architecture, deformation or collapse structures, and to investigate the possibility of the presence of remnants of buried ice.

The basic principles of GPR surveying are that electromagnetic waves travel at different velocities dependent on the electrical and magnetic properties of the earth materials, and that incident waves are refracted or reflected on interfaces between materials with contrasting dielectric permittivities. The nature of the signal that is returned to the surface (i.e. its intensity, polarity and propagation velocity) can then be analysed using processing software (ReflexW; cf. Sandmeier, 2012) which allows the reconstruction and modelling of the architecture of the subsurface.

Fig. 6 shows the survey plan with a single E-W profile capturing the length of the depression, and three shorter N-S profiles across the depression. Data were collected as a continuous array with additional transects surveyed to connect the long and cross profiles (the radar

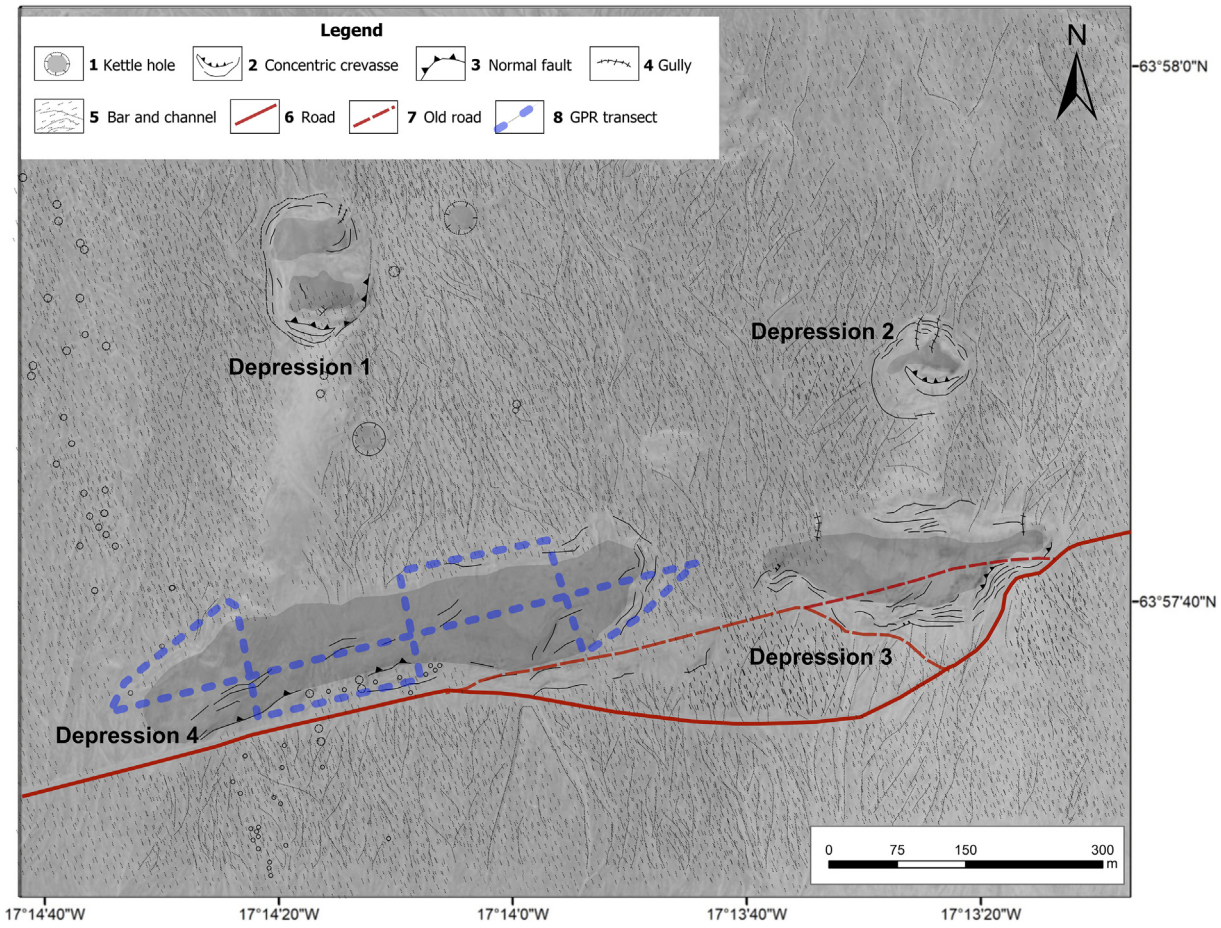

Fig. 6. Geomorphological map of depressions and GPR transects (dashed blue lines). Red broken line represents the original course of a gravel road that has been re-routed to the south due to on-going subsidence of depression. (For interpretation of the references to colour in this figure legend, the reader is referred to the web version of this article.)

profiles outside the depression were used for reference only). Assuming an average propagation velocity of c. 0.07 m ns^{-1} (cf. Cassidy et al., 2003), depth penetration in the sandur sediments was c. 30 m. This is a value typical for velocities in wet, sandy to gravelly materials and may be an underestimation in case of significant quantities of buried ice present in the subsurface.

4. Results

4.1. Morphology of Harðaskriða depressions

All depression measurements are based on their 2007 dimensions. Depression 1 is approximately oval in shape and ranges in width from 164 m (north-south) to 108 m (east-west) (Figs. 7 and 8). The northern and southern rims are characterised by outwardly dipping arcuate and concentric normal faults. Along the southern rim, normal faulting has resulted in the rotation of two large blocks (up to 60 m in length and 15 m wide). The base of this depression is characterised by sagging, uneven terrain, and is divided into two portions of unequal depth. The northernmost part of the depression measured 10 ± 1.64 m in depth, while the southern part of the depression measured 12 ± 1.64 m in depth. Recent satellite imagery (DigitalGlobe, 2016) indicates further depression widening attributed to continued melt-out.

Depression 2 is approximately circular in shape and ranges in width from 89 m (north-south) to 104 m (east-west) and 13 ± 1.64 m deep (Fig. 7). The northern portion contains concentric normal faults and two extensional faults that trend north-south (40 m and 50 m in length). Along the southernmost rim of this depression, normal faulting has resulted in the rotation of two blocks, the largest 60 m long and 13 m wide.

Depression 3 possesses an irregular, elongate morphology that trends east-west. The depression ranges in width from 342 m (east-west) and 116 m (north-south) and is 12 ± 1.64 m deep (Fig. 7). The margin, while not circular in shape, contains numerous normal faults and recesses that surround the depression. The southern margin is marked by several rotated blocks and steep walls. The margin appears to slump in rotational blocks towards the centre, resulting in 'steps' that dip outwards from the depression. A dirt road observed on the 1945 aerial photographs remains visible on the 2007 aerial photographs. Its original surface, although now undulating, remains discernible as it traverses depression 3, suggesting that subsidence has been gradual in nature.

Depression 4, the widest of the depressions, is similar in shape to depression 3, possessing an irregular shape and trending east-west (Fig. 7). The depression ranges in width from 604 m (east-west) to 148 m (north-south). Similar to the other depressions, the walls are steepest along the southern margin, and the margin is characterised by horst and graben blocks and concentric extensional fractures (Figs. 5a, b and 6). Numerous recesses have developed along the northern, eastern and western margin and possess a relatively gentle, stepped slope, compared to those along the steeper southern margin.

Directly 800 m north of these depressions and visible on the 1965 photographs are three drumlinised, elongate ridges that lead to the elevated sandur (Fig. 9a). These ridges trend north-south and, from east to west, are 176 m, 79 m and 151 m in length and 30, 37, and 34 ± 1.64 m in height respectively. Elevation profiles were extracted

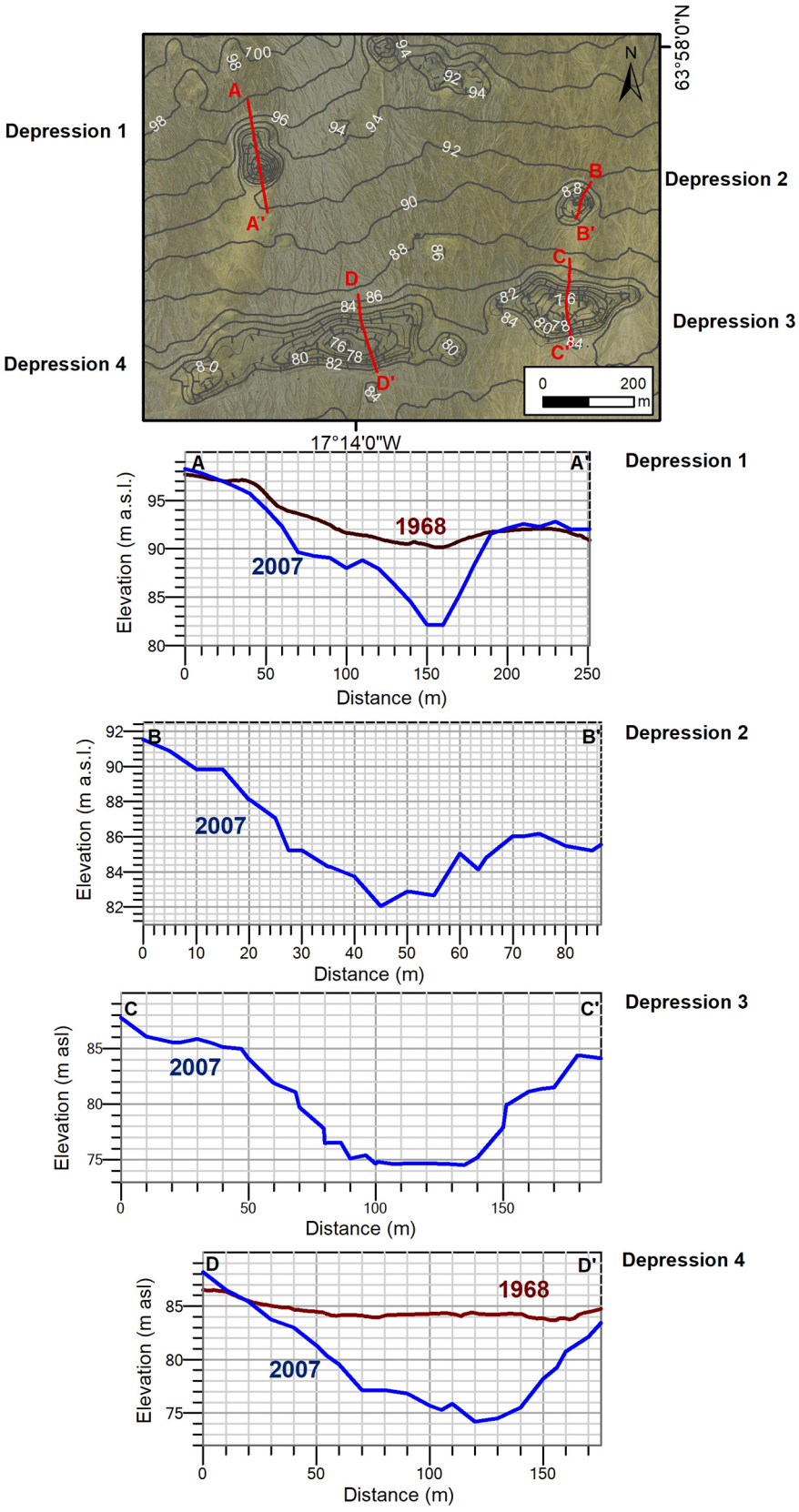

Fig. 7. Profiles of depressions 1–4 in 2007 (dGPS survey transects) are shown in blue; the 1968 surfaces, when available, are shown in red. (For interpretation of the references to colour in this figure legend, the reader is referred to the web version of this article.)

of the area immediately adjacent to these ridges (Profile 1) and the prominent ridges (Profiles 2–4) that rose towards the elevated sandur surface (Fig. 9b). While varying in height, the ridges all span an average of 33 m from the base of the depression to the sandur. Later photo series (1965–1997) indicate that these ridges were largely removed by the fluvial erosion of shifting proglacial

Table 2
Average height difference between DEM and control (check) points surveyed at the field site with error estimates given as root mean square (RMS) errors. Random errors are reported at the 95th percentile limit (all units are in metres). Note '*' designates 1997 and 2003 Loftmyndir DEMs compared with field data.

Photo year	Ave Z dif (m)	RMS (m)	SD (m)	95% confidence (2 × SD) (m)
1965	0.0773	3.4536	3.6062	7.2124
1968	1.8190	2.5760	1.8769	3.7538
1997*	1.5005	2.7248	2.3369	4.6738
2003*	−0.9224	2.7059	2.6221	5.2442
2007	0.1575	1.6187	1.6442	3.2884

drainage channels and by the November 1996 jökulhlaup. The sedimentary section revealed by erosion during the November 1996 jökulhlaup shows a number of large ice blocks up to 30 m in diameter contained within stratified coarse grained jökulhlaup deposits (Fig. 10). Vertical lowering of 12 ± 1.64 m over the 62 years since 1947 was calculated from the height difference between the 1945 and 2007 sandur surfaces, representing an average rate of 19.4 ± 2.6 cm of lowering per year (Figs. 7 and 8).

4.2. Sub-surface structure of Harðaskriða depressions

Using a relatively low radar frequency, and assuming that the subsurface sediment mostly comprises sand and small to medium gravel (with no outsized boulders to cause 'disruptive' hyperbolae) it may be expected that the signal-to-noise ratio is adequate for resolving metre-scale sandur sedimentology down to a depth of c. 30 m.

There are two main sub-horizontal reflectors in the GPR cross-profiles: one at an estimated depth of 6 m and one at c. 20 m below the surface (white solid lines in Fig. 11). A third discontinuous reflector is visible just above the noise which starts at 30 m. As it is right at the detection limit, interpreting this reflector will not be attempted below. The 6 m reflector tends to mirror the surface topography and the 20 m reflector is generally less undulating and continuous across the depression. All three profiles also show shorter sub horizontal reflectors that are thought to represent prominent bedding surfaces. Northward dipping reflectors, a single one in the central cross-profile and two parallel features in the east cross-profile (white dashed lines in Fig. 11), appear to extend down from the 6 m reflector, cross and deflect the 20 m reflector and then connect in a stepped fashion with the reflector at 30 m depth. (See Fig. 12.)

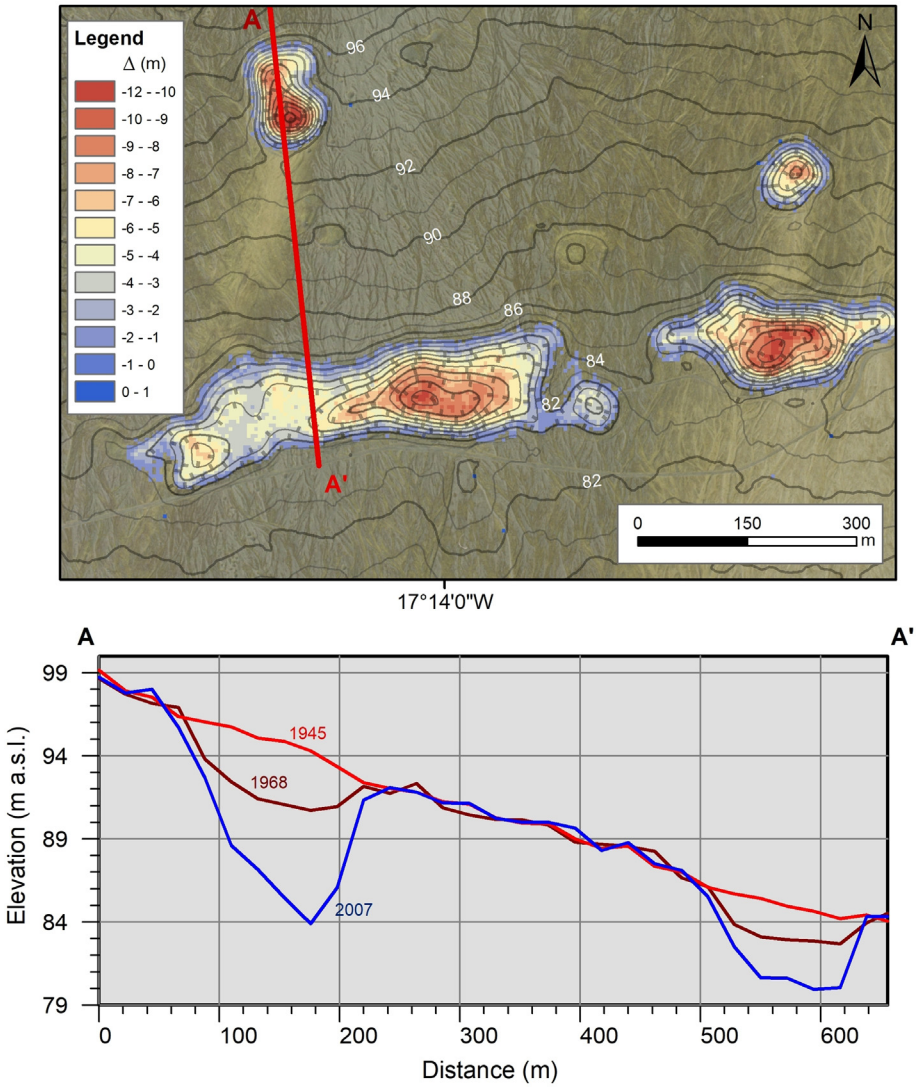

Fig. 8. Total elevation loss (m) between 1945 and 2007 and estimated volume loss estimated by using an artificial 1945 surface (top); profiles of depressions between 1945 (red), 1968 (brown) and 2007 (blue) (bottom). (For interpretation of the references to colour in this figure legend, the reader is referred to the web version of this article.)

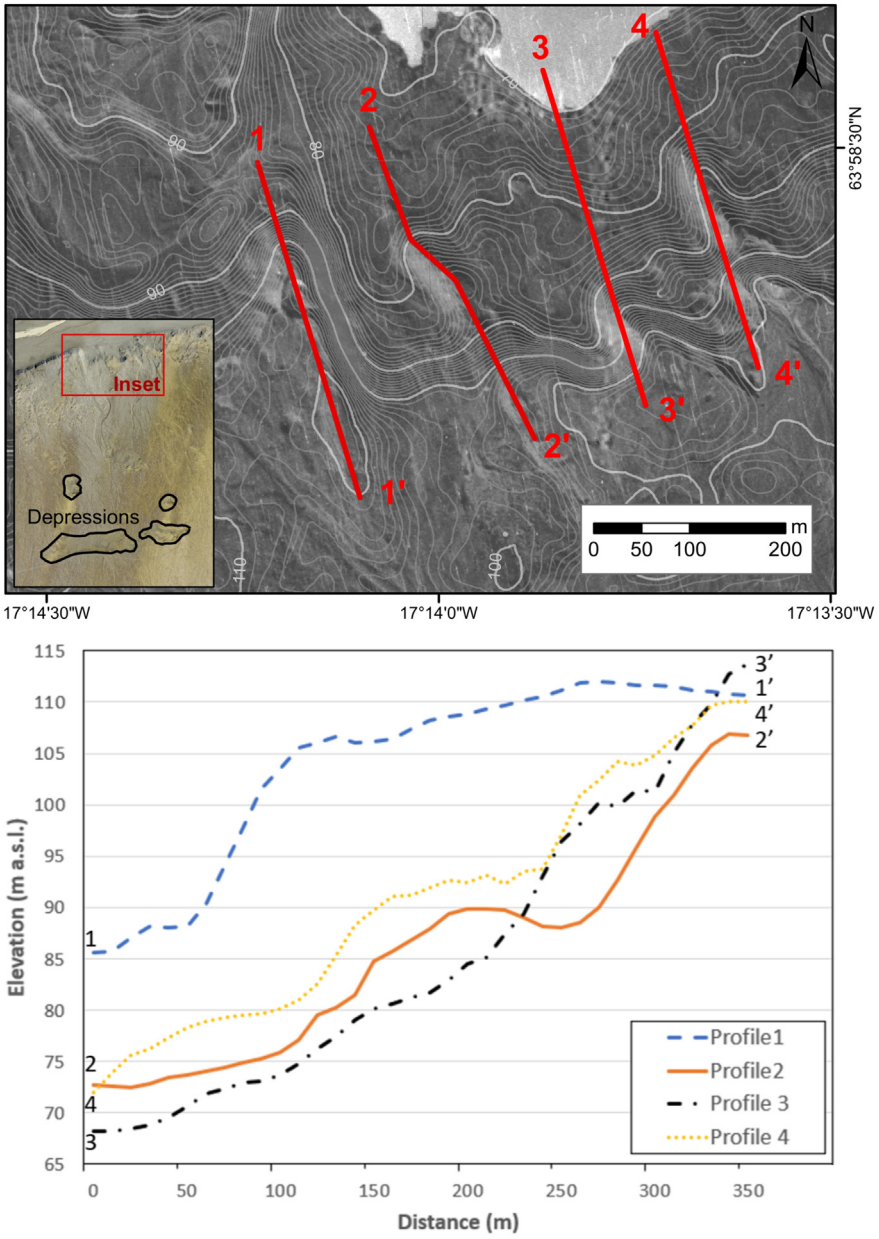

Fig. 9. (a) The location 1965 drumlinised ridges exposed by the retreat of the glacier margin since 1945. (b) Elevation profile of the proglacial depression (profile 1) and drumlinised ridges (profiles 2–4).

In all three cross-profiles, high-angle linear or curvilinear structures (indicated in red in Fig. 11) intersect, or terminate onto the aforementioned reflectors. They are interpreted as joints or normal faults. Particularly near the margins of the depression, they can be seen to disrupt or offset reflectors. Most structures are outward dipping, but there are also less common, apparently younger, inward-dipping faults. All such fractures seem to have developed to accommodate the flexure in the depression and are attributed to progressive subsidence due to gradual melt-out of buried ice. At the surface around the periphery of the depression, the structures present as stepped ring-structures (Figs. 5a, b and 6), which are very similar to the 'concentric' ring-fractures described for collapsing calderas and other ice-melt phenomena by Branney (1995) and Branney and Gilbert (1995).

Whilst confident about the interpretation of the joint and fault structures, the characterisation of the subsurface materials from the radargrams is more challenging, particularly without the possibility of direct ground truthing. There are good exposures near the Gígjukvísl, 5 km kilometres to the west (see Russell et al., 2001a, 2001b), but they are developed into proglacial surfaces which lack the 'pitted' surfaces diagnostic of jökulhlaup deposits. Fortuitously, the 1996 jökulhlaup cut a 30 m high section into sandur sediments 1.3 km north of the Harðaskriða depressions (Fig. 10) so there is at least some information available on textural heterogeneity of the sandur sediments and the distribution and dimensions of buried ice.

Apart from the aforementioned reflectors, the most conspicuous zones in the GPR profiles are those that seem to be devoid of energy returns. Such zones (indicated in blue in Fig. 11), can be observed mostly away from the centre of the depression and below the 6 m reflector, but there are also a few at greater depths. Assuming that these features are not processing artefacts, they must represent homogeneous materials with a low relative dielectric permittivity ε_r. Where a reflector - mostly that at 6 m depth,

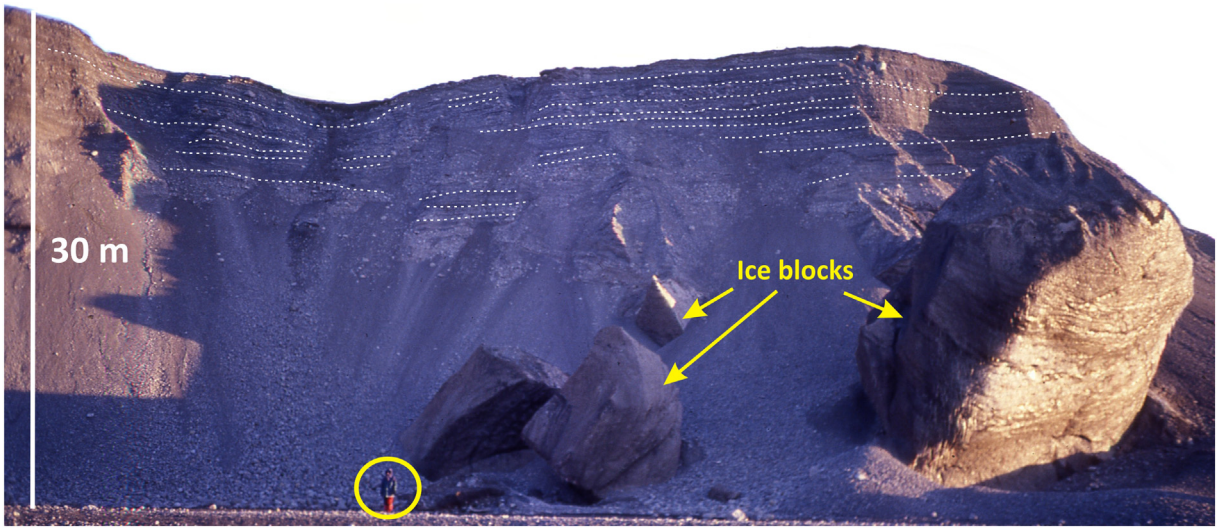

Fig. 10. Photograph taken in May 1997 showing the presence of large isolated blocks of glacier ice within jökulhlaup deposits.

forms the upper surface of such zones - the polarity is opposite to that of the air wave (phase change of 180°) which would suggest that the overlying sediment has a relatively high ε_r. Since ice has an ε_r of 3–4 (Brandt et al., 2007) and overlying materials, which can logically assumed to be relatively (wet) jökulhlaup sediments may be expected to have an ε_r in the order of 10–30 - and drawing analogies with nearby exposures - the zones are tentatively interpreted as remnants of buried ice.

The observation that the interpreted blocks of buried ice are ubiquitous at the north and south sides of the cross-profiles, but less common in the central parts is compatible with the idea that subsidence has been greatest in the centre of the depression. The inward dipping reflector on the south side in the central and east cross-profiles (Fig. 11, middle and lower panels) may delineate the upper surface of relatively intact buried ice. The deeper parts of this surface may have served as a slip-plane extending into one of the deeper identified normal faults.

Although its strength is variable, it is clear that the reflector at 20 m is more continuous than the 6 m reflector. Interestingly, its polarity is the same as the air wave which suggests that it

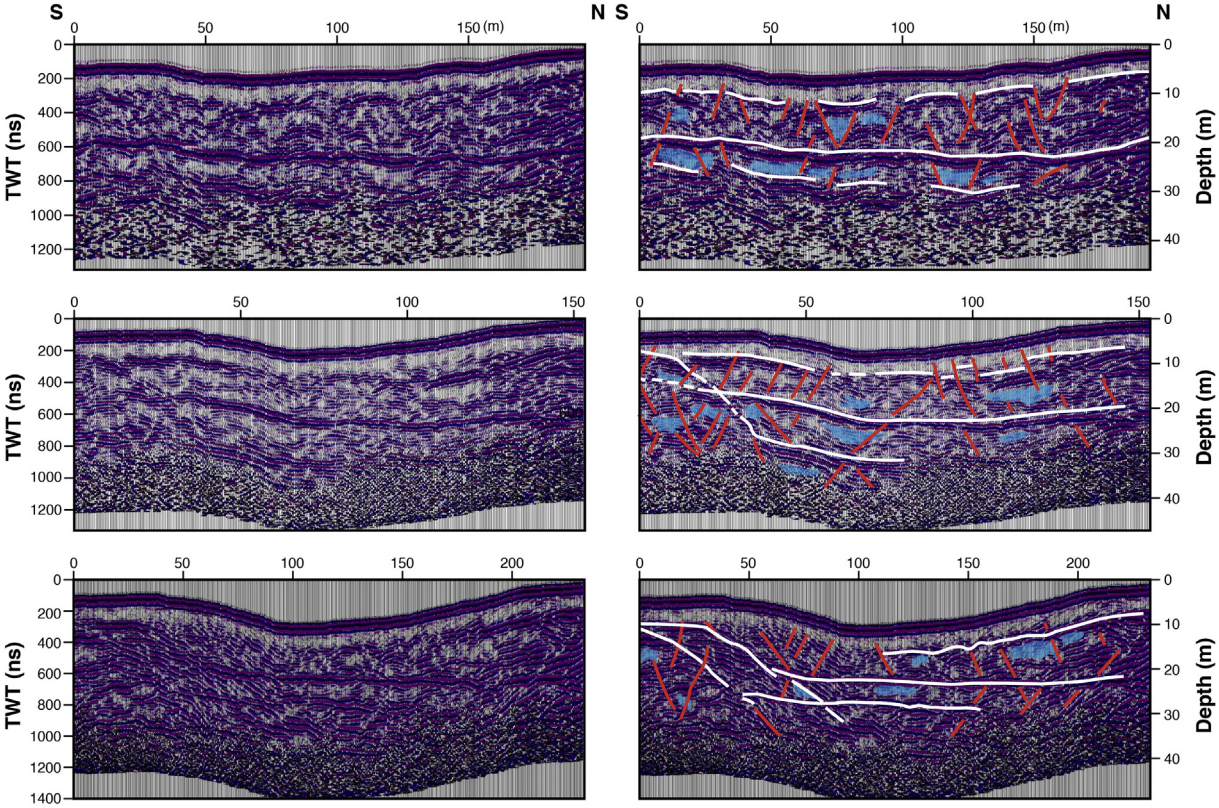

Fig. 11. N-S cross-sectional radargrams through Depression 4. From top to bottom: west line, central line and east line (see Fig. 6). Main reflectors are shown in white, structural features in red, and buried ice remnants in blue. For further explanations, see main text. (For interpretation of the references to colour in this figure legend, the reader is referred to the web version of this article.)

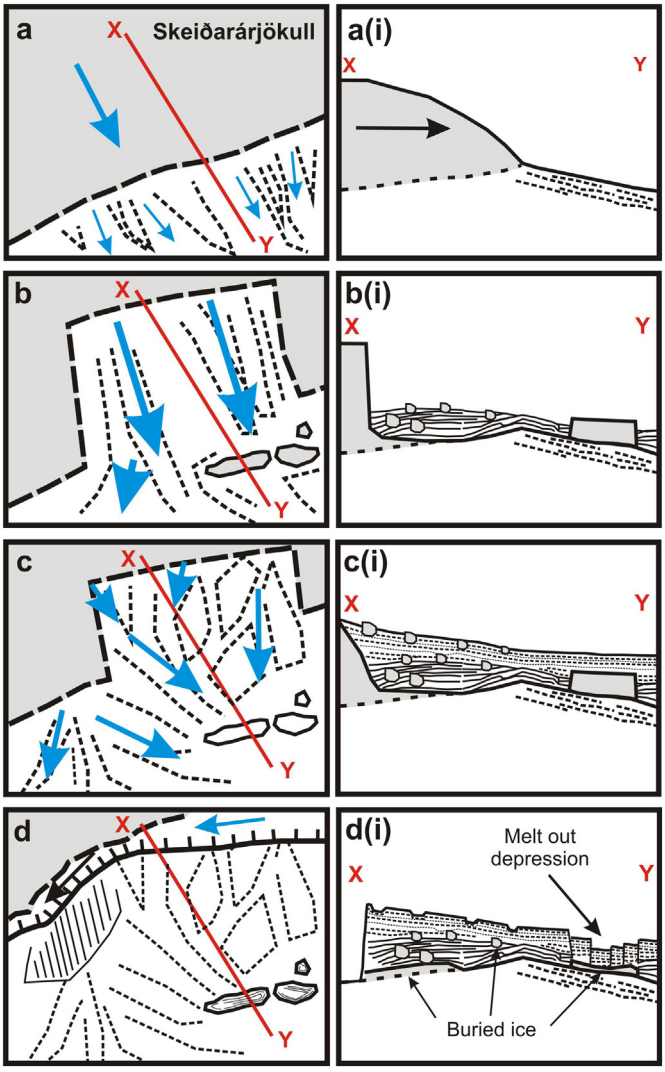

Fig. 12. Model showing the proposed sequence of events responsible for the formation of the Harðaskriða melt out depressions on Skeiðarársandur. (a & ai) Initial glacier position before the 1903 jökulhlaup. (b) Erosion of ice-walled re-entrant into the snout of Skeiðarárjökull during 1903 jökulhlaup and transport of large ice blocks onto sandur. (bi) Partial burial of large 1903 jökulhlaup-transported ice blocks. (c & ci) Burial of 1903 jökulhlaup emplaced ice blocks by 1913 and 1922 jökulhlaup deposits. (d) Glacier margin position in 1945 allows meltwater to drain in a westerly direction along the ice margin abandoning the sandur surface. (di) Abandoned sandur surface showing the presence of isolated buried ice blocks (see Fig. 10) and the development of the large melt out depression.

represents a contact between a lower permittivity (above) to a higher permittivity material below. The fact that it does not show significant offsets where intersected by high angle faults is taken as evidence that the reflector is not a sedimentary surface. Instead it is proposed that it represents the local groundwater table (wet/saturated sand: $\varepsilon_r = 10–30$; Brandt et al., 2007), although it is noted that other studies on the sandur (cf. Cassidy et al., 2003; Burke et al., 2010) have found the groundwater table to be significantly shallower.

5. Discussion

The average rate of 19.4 ± 2.6 cm of lowering per year between 1945 and 2007 determined from this study is an order of magnitude lower than the 1.88 ma^{-1} reported for immediate post jökulhlaup ice-melt out within the Gígjökull basin between 2010 and 2016 (Harrison et al., 2019). Higher buried ice melt rate at Gígjökull can be attributed to the simultaneous deposition of smaller ice fragments with jökulhlaup deposits rather than the melt of large isolated blocks.

Combined DEMs, dGPS measurements and GPR surveys reveal that the Harðaskriða depressions experienced the greatest vertical loss within their centres, due to slump in rotational blocks towards the centres, characteristic of 'horst and graben' structures. This process has resulted in 'steps' that have developed along the side of each of the features into the centre. The concentric rings of normal faulting, horst and graben and normal and extensional faults described at the Harðaskriða depressions 1–4 are consistent with observations made at other field sites involving the melt-out of smaller bodies of ice that have been transported by lahars and jökulhlaups (Maizels, 1992; Branney, 1995; Branney and Gilbert, 1995; Olszewski and Weckwerth, 1999). Such features have also been used as indirect evidence of buried bodies of ice at other locations (e.g. Boulton, 1972; Hambrey, 1984; Krüger and Kjær, 2000; Kjær and Krüger, 2001; Dickson and Head, 2006).

As the ice bodies buried at Harðaskriða began to melt, the loss of volume and drainage of subsurface water may have resulted in the subsidence of the overlying sediment (McDonald and Shilts, 1975; Maizels, 1992). This sort of subsidence can produce outwardly-dipping arcuate hairline fractures that can elongate into a ring, causing the subsidence of a coherent block of sediment as seen in depressions 1 and 2 (Branney, 1995; Branney and Gilbert, 1995). These overhanging scarps become unstable and collapse along new arcuate faults, resulting in the development of extensional crevasses that may continue to expand along small vertical and normal faults causing some walls to collapse, resulting in keystone graben (Sanford, 1959; McDonald and Shilts, 1975). Continued collapse leads to intersection of arcuate fractures resulting in blocks that tilt and subside into the pit, while mass movements and slumping may accelerate the melting rate of a buried ice body (Johnson, 1992).

At larger collapse pits, such as depressions 3 and 4, irregular topographic margins with embayments also developed (Branney, 1995; Branney and Gilbert, 1995). These features, combined with the steep walls of the depressions and undisturbed nature of the surrounding outwash plain are consistent with bodies of ice that have been surrounded by sediment (Maizels, 1991). The gentle slopes of the northern walls and the steeper slopes of the southern walls are consistent with the development of a 'normal' kettle hole (Maizels, 1992; Olszewski and Weckwerth, 1999), as proglacial outwash would have resulted in the development of gravitational flow on the northern side, while block displacement and subsidence developed on the southern side following melt out.

The existence of large bodies of buried ice >30 m in thickness on Skeiðarársandur have been identified and documented using resistivity studies (Everest and Bradwell, 2003) and confirmed at exposures (Klimek, 1972; Bogacki, 1973; Churski, 1973; Jewtuchowicz, 1973; Russell and Knudsen, 1999; Molewski, 2000). Ridges and detached slabs of dead ice in the eastern and western parts of Skeiðarársandur have also been identified and described and are attributed to deposition by the retreating ice margin (Galon, 1973; Jewtuchowicz, 1973; Wojcik, 1973). Unlike ice-cored ridges, plains or moraines elsewhere on the sandur, the geometry, orientation and size of the bodies of ice that resulted in the Harðaskriða depressions are consistent with other descriptions of isolated blocks of ice emplaced during high-magnitude jökulhlaups (Maizels, 1992; Maizels and Russell, 1992; Branney, 1995; Branney and Gilbert, 1995; Harrison et al., 2019).

A topographic map published in 1904 (Danish Staff Map) depicts several elongated, east-west trending ridges extending across central Skeiðarársandur that appear to be continuations of the 19th century moraines that persist today in the western region of the sandur (Fig. 2). By 1945, aerial photographs reveal that these moraines are no longer visible on the central sandur, and reportedly buried or removed by jökulhlaups (Galon, 1973; Jewtuchowicz, 1973; Wojcik, 1973; Wisniewski et al., 1997; Knudsen et al., 2001). While some of the

depressions and landforms correspond to the approximate positions of the 19th century moraines, the largest Harðaskriða depressions are developed approximately 400 m south of this limit, suggesting that they are not related to buried ice bodies contained within the pre-existing 19th century moraines (Fig. 4).

According to Thórarinsson (1974), a large piece of the glacier margin detached during the 1903 jökulhlaup approximately 1 km in length and up to 150 m in height; it was also documented that a fracture of similar size and length developed up glacier located where the floodwaters burst from the glacier margin. During this same flood, house-size ice blocks were emplaced on the sandur and the flood waters *"dug into the sand a deep, 'many persons high', steep-sided channel"* (Thórarinsson, 1974). Ice blocks, regardless of their original shapes, result in circular depressions, such as Depression 2, however dumbbell-shaped pits may form where circular collapse pits from two closely adjacent buried blocks of ice overlap, such as Depression 1 (Branney and Gilbert, 1995). The geometry and orientation of the largest elongated depressions (Depressions 3 and 4) may therefore correspond to the 1 km wide portion of the margin that was detached during the 1903 jökulhlaup described by Thórarinsson (1974). In the absence of evidence of a disrupted glacier snout or ice blocks on the topographic map published in 1904, it is presumed that the field survey that formed the basis for this map pre-dated the 1903 jökulhlaup.

Thórarinsson (1974) stated that jökulhlaups in 1913 and 1922 inundated the central sandur with floodwaters and sediment. During later periods of glacier stillstand, meltwater runoff was concentrated in the central part of the sandur, resulting in the formation of wide outwash channels (Galon, 1973). In common with glacier termini elsewhere in Iceland, the margin of Skeiðarárjökull experienced climate-forced recession from their Little Ice Age maximum extents (Thórarinsson, 1943; Sigurðsson, 2005). Recession of Skeiðarárjökull resulted in meltwater drainage from the glacier margin at progressively lower elevations leading to sandur incision (Galon, 1973). As such, subsequent jökulhlaups in 1934 and 1938 did not affect Harðaskriða, as the floodwaters were routed through other channels such as the Háöldukvísl, 1.5 km to the east (Fig. 1). Aerial photographs taken in 1945 show the formation of a proglacial trench and meltwater flow in a westerly direction towards the Gígjukvísl (Figs. 1 and 3).

While the jökulhlaup-transported ice bodies may have been emplaced as early as 1897 and as late as 1922, any melting that occurred during that time is not captured due to a lack of available imagery. The rate of melt of a buried ice body may be affected by a variety of factors, including the amount of sediment within the ice, depth of burial and geothermal heat flux (Nakawo and Young, 1981; Nicholson and Benn, 2006), making it difficult to estimate the initial size of the buried ice body. Ice blocks emplaced and completely buried by the 1903 jökulhlaup would have been further insulated by additional sediment aggradation during the 1913 and 1922 jökulhlaups (Thórarinsson, 1974). That glacier ice buried by November 1996 jökulhlaup deposits has survived for 23 years illustrates the feasibility of buried ice preservation between the 1903 and 1913 jökulhlaups.

It is noticeable that the Harðaskriða depressions are not visible on the 1945 photographs, suggesting that the buried ice has not exhibited high melting rates. It is not until the 1965 photographs, following the retreat of the central lobe of the glacier margin and the subsequent formation of the proglacial trench post-1945, that subsidence is visible. This observation and the sequence of events presented in this study suggests that the melt rate of the buried ice bodies may have been accelerated as a result of the retreat and decoupling of the glacier margin and the associated rise in ambient temperatures and lowering of local groundwater table (Robinson et al., 2008; Levy et al., 2015). This demonstrates the control that glacier margin stability has on post-depositional modification processes, as buried ice bodies may be capable of persisting for much longer periods at a stable or advancing margin, characterised by proglacial aggradation, rather than at a retreating or stagnating margin characterised by proglacial incision.

According to Björnsson et al. (1999) profiles of the surface of Skeiðarárjökull in 1904 were ~100 m higher than in 1945, which would have resulted in a steeper ice surface gradient and therefore increased hydraulic gradient during high-magnitude jökulhlaups (Roberts et al., 2000, 2001; Roberts, 2005). This would have increased the capacity of jökulhlaups to excavate and transport sediment. The elongate, drumlinised ridges observed on the 1965 images on the down-glacier side of the proglacial trench generated by the retreat of the glacier margin are interpreted as conduit-fill eskers created by sediment deposition as meltwater ascended by at least 30 m over a distance of ~200 m from the proglacial depression to innundate Harðaskriða (Fig. 9).

The landform and sediment assemblage at Harðaskriða reflect the role of multiple jökulhlaups just after the Little Ice Age maximum extent of Skeiðarárjökull. Initial glacier position before the 1903 jökulhlaup is associated with unconfined proglacial drainage (Russell and Knudsen, 1999, 2002; Russell et al., 2005, 2006) (Fig. 12a and a(i). Erosion of a 1 km wide ice-walled re-entrant into the snout of Skeiðarárjökull by the 1903 jökulhlaup liberated large ice blocks which were transported by the jökulhlaup onto the sandur for distances of up to 0.5–0.8 km (Fig. 12b). The largest 1903 jökulhlaup-transported ice blocks were probably partially buried as was the case with the largest ice blocks during the 1996 jökulhlaup (Russell and Knudsen, 1999; Fay, 2001, 2002a) (Fig. 12b(i). Sediment aggradation during the 1913 and 1922 jökulhlaups buried the ice blocks emplaced in 1903 (Fig. 12c(i). It is likely that the ice blocks had reduced in size by ablation between 1903 and 1913. Continued glacier recession resulted in the abandonment of the Harðaskriða sandur surface between 1933 and 1945 (Fig. 12d). Melt of buried ice results in depressions which have deepened and expanded in surface area between 1968 and 2007 (Fig. 12d (i). The GPR survey undertaken in 2013 of the largest depression indicates the presence of buried glacier ice which together with the recent satellite observations of depression widening, suggests that the melt out processes are ongoing.

6. Conclusions

Continued melting of the Harðaskriða ice bodies nearly a century following their emplacement and burial demonstrates that jökulhlaups may continue to be an important control on sandur evolution over decadal to centennial timescales (10^1–10^2 years). Buried ice meltout associated with the development of the Harðaskriða depressions was enhanced by the lowering of the groundwater table following abandonment of the sandur brought about by glacier margin recession during the second half of the twentieth century. The occurrence of three high magnitude jökulhlaups within an 18-year period following the Little Ice Age glacier maximum extent resulted in significant sandur aggradation and ice block burial, assisting the long term preservation of ice. By contrast, a similar succession of jökulhlaups during a period of glacier margin recession will reduce the potential for jökulhlaup-transported ice blocks to be buried as repeated 'decoupling' of the glacier margin from the its sandur reduces the potential for stacking of jökulhlaup deposits.

Our model of the jökulhlaup landsystem at Harðaskriða and the ability to identify them at other warm-based sediment-rich glaciers that may be subject to some or all the large-scale processes including margin fluctuations, jökulhlaup dynamics and secondary modification may provide a useful analogue for interpreting landforms and strata emplaced by margin fluctuations, jökulhlaups and melt out generated by the retreating continental Pleistocene ice sheets.

Declaration of competing interest

The authors declare that they have no known competing financial interests or personal relationships that could have appeared to influence the work reported in this paper.

Acknowledgements

AJR, DJB, ARGL and FST acknowledge the Earthwatch Institute for fieldwork funding. AJR and ARGL thank the NERC ARSF (IPY07/13) for acquisition of 2007 aerial photography and AJR's fieldwork in 1996-97 was funded by (GR3/10960). We thank Ragnar Frank Kristjánsson and Regína Hreinsdóttir for valuable support for jökulhlaup-related research within Skaftafell/Vatnajökull National Park. We thank Marek Ewertowski for acquiring the 2013 GPS data and Chris Williams for conducting the topographic corrections of the GPR data. We thank Anders Schomacker and an anonymous reviewer for their constructive comments on this paper. Achim Belich is thanked for editorial oversight. Thanks to Salvatore G. Candela for assistance with digital elevation models.

References

Baily, B., Collier, P., Farres, P., Inkpen, R., Pearson, A., 2003. Comparative assessment of analytical and digital photogrammetric methods in the construction of DEMS and geomorphological forms. Earth Surf. Process. Landf. 28, 307–320.
Ballantyne, C.K., 2002. Paraglacial Geomorphology. Quat. Sci. Rev. 21 (18–19), 1935–2017.
Bennett, M.R., Glasser, N.F., 2009. Glacial Geology: Ice Sheets and Landforms. Second edition. Wiley-Blackwell, Oxford 385pp.
Björnsson, H., 1992. Jökulhlaups in Iceland: prediction, characteristics and simulation. Ann. Glaciol. 16, 95–106.
Björnsson, H., 1997. Grímsvatnahlaup Fyrr og Nu. In: Haraldsson, H. (Ed.), Vatnajökull: Gos og hlaup 1996. Reykjavík, Vegagerðin, pp. 61–77.
Björnsson, H., 1998. Hydrological characteristics of the drainage system beneath a surging glacier. Nature 395, 771–774.
Björnsson, H., Pálsson, F., Magnússon, E., 1999. Skeiðarárjökull: Landslag og rennslisleiður vatns undir sporði. Raunvísindastofnun Háslólans. RH-11-1999.
Blauvelt, D., 2013. Evolution of a Sandur: sixty years of change, Skeiðarársandur, Iceland. PhD Thesis, Newcastle University, 301pp.
Bogacki, M., 1973. Geomorphological and geological analysis of the proglacial area of Skeiðarárjökull. Central, western and eastern sections, Geographia Polonica 26, 57–88.
Boulton, G.S., 1972. Modern Arctic glaciers as depositional models for former ice sheets. J. Geol. Soc. Lond. 128, 361–393.
Brandt, O., Langley, K., Kohler, J., Hamran, S.E., 2007. Detection of buried ice and sediment layers in permafrost using multi-frequency Ground Penetrating Radar: a case examination on Svalbard. Remote Sensing in the Environment 111, 212–227.
Branney, M.J., 1995. Downsag and extension at calderas: new perspectives on collapse geometries from ice-melt, mining and volcanic subsidence. Bull. Volcanol. 57, 303–318.
Branney, M.J., Gilbert, J.S., 1995. Ice-melt collapse pits and associated features in the 1991 lahar deposits of Volcan Hudson, Chile: criteria to distinguish eruption-induced glacier melt. Bull. Volcanol. 57, 293–302.
Burke, M.J., Woodward, J., Russell, A.J., Fleisher, P.J., Bailey, P.K., 2010. The sedimentary architecture of outburst flood eskers: a comparison of ground-penetrating radar from Bering Glacier, Alaska and Skeiðarárjökull, Iceland. GSA Bull. 122 (9–10), 1637–1645.
Cassidy, N.J., Russell, A.J., Marren, P.M., Fay, H., Rushmer, E.L., Van Dijk, T.A.G.P., Knudsen, Ó., 2003. GPR-derived architecture of November 1996 jökulhlaup deposits, Skeiðarársandur, Iceland. In: Bristow, C.S., Jol, H.M. (Eds.), Ground Penetrating Radar in Sedimentation. Spec. Publ. Geol. Soc. 211, pp. 153–166.
Churski, Z., 1973. Hydrographic features of the proglacial area of Skeiðarárjökull. Geogr. Pol. 26, 209–254.
Dickson, J., Head, J.W., 2006. Evidence for an Hesperian-aged South circum-Polar lake margin environment on Mars. Planetary and Space Science 54, 251–272.
Douglas, T.D., Harrison, S., 1996. Turf-banked terraces in Öræfi, southeast Iceland: morphology, rates of movement, and environmental controls. Arct. Alp. Res. 28, 228–236.
Evans, D.J.A., England, J., 1992. Geomorphological evidence of Holocene climate change from northwest Ellesmere Island, Canadian High Arctic. Holocene 2, 148–158.
Evans, D.J.A., Twigg, D.R., 2002. The active temperate glacial landsystem: a model based on Breiðamerkurjökull and Fjallsjökull, Iceland. Quat. Sci. Rev. 21 (20–22), 2143–2177.
Evans, D.J.A., Lemmen, D.S., Rea, B.R., 1999. Glacial landsystems of the southwest Laurentide Ice Sheet: modern Icelandic analogues. Geomorphology 14, 673–691.
Evans, D.J.A., Ewertowski, M.W., Orton, C., 2019. The glacial landsystem of Hoffellsjökull, SE Iceland: contrasting geomorphological signatures of active temperate glacier recession driven by ice lobe and bed morphology. Geogr. Ann. 101A, 249–276.
Everest, J., Bradwell, T., 2003. Buried glacier ice in southern Iceland and its wider significance. Geomorphology 52, 347–358.
Eyles, N., Boyce, J.I., Barendregt, R.W., 1999. Hummocky moraine: sedimentary record of stagnant Laurentide Ice Sheet lobes resting on soft beds. Sediment. Geol. 123 (3–4), 163–174.
Fard, A.M., 2003. Large dead-ice depressions in flat-topped eskers: evidence of a Preboreal jökulhlaup in the Stockholm area, Sweden. Glob. Planet. Chang. 35 (3–4), 273–295.
Fay, H., 2001. The role of ice blocks in the creation of distinctive proglacial landscapes during and following glacier outburst floods (jökulhlaups). PhD thesis, Keele University.
Fay, H., 2002a. Formation of ice-block obstacle marks during the November 1996 glacier-outburst flood (jökulhlaup), Skeiðarársandur, southern Iceland. In: Martini, I.P., Baker, V.R., Garzon, G. (Eds.), Flood and Megaflood Processes and Deposits: Recent and Ancient Examples. International Association of Sedimentologists Special Publication 32, pp. 85–97.
Fay, H., 2002b. Formation of kettle holes following a glacial outburst flood (jökulhlaup), Skeiðarársandur, southern Iceland. in: Snorasson, A., Finnsdóttir, H.P., Moss, M., (Eds.) The Extremes of the Extremes: Extraordinary Floods. Proceedings of a symposium held at Reykjavik, Iceland, July 2000. IAHS Publication Number 271, pp. 205-210.
French, H.M., Harry, D.G., 1990. Observations on buried ice and massive segregated ice, western arctic coast, Canada. Permafr. Periglac. Process. 1, 31–43.
Galon, R., 1973. Geomorphological and geological analysis of the proglacial area of Skeiðarárjökull: central section. Geogr. Pol. 26, 15–57.
Glacier risks database, 2005. http://www.nimbus.it/glaciorisk/gridabasemainmenu.asp (Accessed 25/04/2019).
Hambrey, M.J., 1984. Sedimentary processes and buried ice phenomena in the proglacial areas of Spitsbergen glaciers. J. Glaciol. 30, 104,116–119.
Harrison, D., Ross, N., Russell, A.J., Dunning, S.A., 2019. Post-jökulhlaup geomorphic evolution of the Gígjökull Basin, Iceland. Ann. Glaciol. 60 (80), 1–11.
Ives, J.D., 2007. Skaftafell in Iceland: A Thousand Years of Change. Reykjavik, Ormstunga 256pp.
Jewtuchowicz, S., 1973. The present-day marginal zone of Skeiðarárjökull. Geogr. Pol. 26, 115–138.
Johnson, P.G., 1992. Stagnant glacier ice, St. Elias Mountains, Yukon. Geogr. Ann. 74A (1), 13–19.
Kjær, K.H., Krüger, J., 2001. The final phase of dead-ice moraine development: processes and sediment architecture, Kötlujökull, Iceland. Sedimentology 48, 935–952.
Kleman, J., 1992. The palimpsest glacial landscape in northwestern Sweden. Late Weichselian deglaciation landforms and traces of older west-centered ice sheets. Geogr. Ann. 74A (4), 305–325.
Kleman, J., Stroeven, A.P., 1997. Preglacial surface remnants and Quaternary glacial regimes in northwestern Sweden. Geomorphology 19 (1–2), 35–54.
Klimek, K., 1972. Present-day fluvial processes and relief of Skeiðarársandur plain (Iceland). Polska Academia Nauk Institut Geografi 94, 129–139.
Knudsen, Ó., Jóhannesson, H., Russell, A.J., Haraldsson, H., 2001. Changes in the Gígjukvísl river channel during the November 1996 jökulhlaup. Skeiðarársandur, Iceland, Jökull 50, 19–32.
Korsgaard, N.J., Schomacker, A., Benediktsson, Í.Ö., Larsen,N.K., Ingólfsson,Ó., Kjær, K.H. 2015. Spatial distribution of erosion and deposition during a glacier surge: Brúarjökull, Iceland. Geomorphology 250, 258–270.
Krüger, J., 1994. Glacial processes, sediments, landforms and stratigraphy in the terminus region of Mýrdalsjökull, Iceland. Folia Geogr. Dan. 21, 1–233.
Krüger, J., Kjær, K.H., 2000. De-icing progression of ice-cored moraine in a humid, subpolar climate, Kötlujökull, Iceland. Holocene 10, 721–731.
Levy, A., Robinson, Z., Krause, S., Waller, R., Weatherill, J., 2015. Long-term variability of proglacial groundwater-fed hydrological systems in an area of glacier retreat, Skeiðarársandur, Iceland. Earth Surf. Process. Landf. 40, 981–994.
Lister, H., 1953. Report on glaciology at Breiðamerkurjökull, 1951. Jökull 1, 23–31.
Lukas, S., Nicholson, L.I., Ross, F.H., Humlum, O., 2005. Formation, meltout processes and landscape alteration of High-Arctic ice-cored moraines-examples from Nordenskiold Land, Central Spitsbergen. Polar Geogr. 29, 157–187.
Maizels, J.K., 1991. Origin and evolution of Holocene sandurs in areas of jökulhlaup drainage, South Iceland. In: Maizels, J.K., Caseldine, C. (Eds.), Environmental Change in Iceland: Past and Present. Kluwer, Dordrecht, pp. 267–300.
Maizels, J.K., 1992. Boulder ring structures produced during jökulhlaup flows-origin and hydraulic significance. Geogr. Ann. 74A, 21–33.
Maizels, J.K., Russell, A.J., 1992. Quaternary perspectives on jökulhlaup prediction. In: Gray, J.M. (Ed.), Applications of Quaternary Research. Quaternary Proceedings 2, pp. 133–153.
McDonald, B.C., Shilts, W.W., 1975. Interpretation of faults in glaciofluvial sediments. In: Jopling, A.V., McDonald, B.C. (Eds.), Glaciofluvial and glaciolacustrine sedimentation. SEPM Special Publication 23, pp. 123–131.
McKenzie, G.D., 1969. Observations on a collapsing kame terrace in Glacier Bay National Monument, southeast Alaska. J. Glaciol. 8, 413–414.
Nakawo, M., Young, G.J., 1981. Field experiments to determine the effect of a debris layer on ablation of glacier ice. Ann. Glaciol. 2, 85–91.
Nakawo, M., Young, G.J., 1982. Estimate of glacier ablation under debris layer from surface temperature and meteorological variables. J. Glaciol. 28, 29–34.
Nicholson, L., Benn, D.I., 2006. Calculating ice melt beneath a debris layer using meteorological data. J. Glaciol. 52 (178), 463–470.
Olszewski, A., Weckwerth, P., 1999. The morphogenesis of kettles in the Höfðabrekkujökull forefield, Mýrdalssandur, Iceland. Jökull 47, 71–88.
Østrem, G., 1959. Ice melting under a thin layer of moraine and the existence of ice cores in moraine ridges. Geogr. Ann. 41A, 228–230.
Porter, C., et al., 2018. ArcticDEM https://doi.org/10.7910/DVN/OHHUKH.
Price, R.J., 1969. Moraines, sandar, kames and eskers near Breiðamerkurjökull, Iceland. Trans. Inst. Br. Geogr. 46, 17–43.
Roberts, M.J., 2005. Jökulhlaups: a reassessment of floodwater flow through glaciers. Rev. Geophys. 43, RG1002. https://doi.org/10.1029/2003RG000147.
Roberts, M.J., Russell, A.J., Tweed, F.S., Knudsen, Ó., 2000. Ice fracturing during jökulhlaups; implications for englacial floodwater routing and outlet development. Earth Surf. Process. Landf. 25, 1429–1446.
Roberts, M.J., Russell, A.J., Tweed, F.S., Knudsen, Ó., 2001. Controls on englacial sediment deposition during the November 1996 jökulhlaup, Skeiðarárjökull, Iceland. Earth Surf. Process. Landf. 26, 935–952.
Robinson, Z.P., Fairchild, I.J., Russell, A.J., 2008. Hydrogeological implications of glacial landscape evolution at Skeiðarársandur, SE Iceland. Geomorphology 97, 218–236.

Russell, A.J., Knudsen, Ó., 1999. Controls on the sedimentology of November 1996 jökulhlaup deposits, Skeiðarársandur, Iceland. in: Fluvial Sedimentology VI (ed. by N. D. Smith, & J. Rogers), I.A.S. Spec. Publ. 28, 315–329.
Russell, A.J., Knudsen, Ó., 2002. The effects of glacier-outburst flood flow dynamics on ice-contact deposits: November 1996 jökulhlaup, Skeiðarársandur, Iceland. In: Martini, I. P., Baker, V.R., Garzon, G. (Eds.), Flood and Megaflood Deposits: Recent and Ancient Examples. Blackwell Science, Oxford, pp. 67–83.
Russell, A.J., Knudsen, Ó., Fay, H., Marren, P.M., Heinz, J., Tronicke, J., 2001a. Morphology and sedimentology of a giant supraglacial, ice-walled, jökulhlaup channel, Skeiðarársandur, Iceland. Global Planetary Change 28, 203–226.
Russell, A.J., Knight, P.G., van Dijk, T.A.G.P., 2001b. Glacier surging as a control on the development of proglacial, fluvial landforms and deposits, Skeiðarársandur, Iceland. Glob. Planet. Chang. 28, 163–174.
Russell, A.J. Fay, H., Marren, P.M., Tweed, F.S., Knudsen Ó., 2005. Icelandic jökulhlaup impacts. in: Caseldine, C.J., Russell, A.J., Knudsen, Ó., & Harðardóttir, (eds.) Iceland: Modern Processes and Past Environments. Elsevier Book. pp. 153-204.
Russell, A.J., Roberts, M.J., Fay, H., Marren, P.M., Cassidy, N.J., Tweed, F.S., Harris, T., 2006. Icelandic jökulhlaup impacts: implications for ice-sheet hydrology, sediment transfer and geomorphology. Geomorphology 75, 33–64.
Sandmeier, K.J., 2012. ReflexW 8.1, Program for the Processing of Seismic, Acoustic or Electromagnetic Reflection, Refraction and Transmission Data; Software Manual: Karlsruhe, Germany.
Sanford, A.R., 1959. Analytical and experimental study of simple geologic structures. Geol. Soc. Am. Bull. 70, 19–52.
Schiefer, R., Gilbert, R., 2007. Reconstructing morphometric change in a proglacial landscape using historical aerial photography and automated DEM generation. Geomorphology 88, 167–178.
Schomacker, A., 2008. What controls dead-ice melting under different climate conditions? A discussion. Earth-Sci. Rev. 90 (3–4), 103–113.
Schomacker, A., Kjær, K.H., 2007. Origin and de-icing of multiple generations of ice-cored moraines at Brúarjökull. Iceland. Boreas 36 (4), 411–425.
Sigurðsson, O., 2005. Variations of termini of glaciers in Iceland in recent centuries and their connection with climate. Developments in Quaternary Sciences 5, 241–255.
Snorrason, Á., Jónsson, P., Pálsson, S., Árnason, S., Víkingsson, S., Kaldal, I., 2002. November 1996 jökulhlaup on Skeiðarársandur outwash plain, Iceland. In: Martini, I.P., Baker, V. R., Garzón, G. (Eds.), Flood and Megaflood Processes and Deposits: Recent and Ancient Examples. Special Publication of the International Association of Sedimentologists 32, pp. 55–65.
Thórarinsson, S., 1943. Oscillations of the Iceland Glaciers in the last 250 years. Geogr. Ann. 25A, 1–54.
Thórarinsson, S., 1974. Vötnin Stríð: Saga Skeiðarárhlaupa og Grimsvatnagosa. Bókaútgáfa Menningarsjods, Reykjavik 254p.
Thórhallsdóttir, T.E., 1996. Seasonal and annual dynamics of frozen ground in the central highland of Iceland. Arct. Alp. Res. 28, 237–243.
Tonkin, N., Midgley, N.G., Cook, S.J., Graham, D.J., 2016. Ice-cored moraine degradation mapped and quantified using an unmanned aerial vehicle: a case study from a polythermal glacier in Svalbard. Geomorphology 258, 1–10.
Wisniewski, E., Andrzejewski, L., Molewski, P., 1997. Fluctuations of the snout of Skeiðarárjökull in Iceland in the last 100 years and some of their consequences in the central part of its forefield. Landform Analysis 1, 73–78.
Wojcik, G., 1973. Glaciological studies on the Skeiðarárjökull. Geogr. Pol. 26, 185–208.